

Variable rotational line broadening in the Be star Achernar^{*}

Th. Rivinius¹, D. Baade², R. H. D. Townsend³, A. C. Carciofi⁴, and S. Štefl⁵

¹ ESO — European Organisation for Astron. Research in the Southern Hemisphere, Santiago, Chile, Casilla 19001

² ESO — European Organisation for Astron. Research in the Southern Hemisphere, Garching, Germany, Karl-Schwarzschild-Str. 2

³ Department of Astronomy, Univ. of Wisconsin-Madison, 2535 Sterling Hall, 475 N. Charter Street, Madison, WI 53706, USA

⁴ Instituto de Astronomia, Geofísica e Ciências Atmosféricas, Universidade de São Paulo, 05508-900, São Paulo, SP, Brazil

⁵ ESO/ALMA — The Atacama Large Millimeter/Submillimeter Array, Alonso de Córdova 3107, Vitacura, Santiago, Chile

Received: <date>; accepted: <date>; L^AT_EXed: August 24, 2021

ABSTRACT

Aims. The main theoretical problem for the formation of a Keplerian disk around Be stars is how to supply angular momentum from the star to the disk, even more so since Be stars probably rotate somewhat sub-critically. For instance, nonradial pulsation may transport angular momentum to the stellar surface until (part of) this excess supports the disk formation/replenishment. The nearby Be star Achernar is presently building a new disk and offers an excellent opportunity to observe this process from relatively close-up.

Methods. Spectra from various sources and epochs are scrutinized to identify the salient stellar parameters characterizing the disk life cycle as defined by H α emission. Variable strength of the non-radial pulsation is confirmed, but does not affect the further results.

Results. For the first time it is demonstrated that the photospheric line width does vary in a Be star, by as much as $\Delta v \sin i \lesssim 35 \text{ km s}^{-1}$. However, contrary to assumptions in which a photospheric spin-up accumulates during the diskless phase and then is released into the disk as it is fed, the apparent photospheric spin-up is positively correlated with the appearance of H α line emission: The photospheric line widths and circumstellar emission increase together, and the apparent stellar rotation declines to the value at quiescence after the H α line emission becomes undetectable.

Key words. Line: profiles – Stars: rotation – emission-line, Be – individual: α Eri

1. Introduction

Be stars are rapidly rotating stars that form gaseous, circumstellar viscous decretion disks (see Rivinius et al. 2013a, for a review). In order to form a viscous decretion disk and keep it in existence, angular momentum must be supplied to the inner part of the disk, which is then transported outwards by viscosity (see, e.g., Haubois et al. 2012). It is generally considered that Be stars rotate close to, but not at critical value, so that there has to be a disk formation process acting on top of the rotation. Since in many Be stars the disk is transient, either the formation or the dissipation process of the disk, or both, must be able to vary with time in efficiency for a given star. Among the proposed mechanisms for this is the pulsational build-up of excess angular momentum in the upper photosphere that eventually “of-floods” into a circumstellar disk (Ando 1986; Rogers et al. 2013; Neiner et al. 2013). Such a mechanism should leave an imprint on the photosphere by increasing the rotational line widths, usually expressed as $v \sin i$, before the disk is formed/supplied with angular momentum, and then should decrease as the disk forms. To our knowledge, no observational results from searching for such a phenomenon have been published.

The southern Be star Achernar (α Eri, HD 10144) is the apparently brightest Be star. The star is mostly classified as B3 V or B4 IV, but sometimes as well as B6 V. Vinicius et al. (2006) attempted to reconcile these discrepant spectral types and other

published parameter values by taking the rapid rotation of the star into account, and derived a “surface mean effective temperature” of 15 000 K. Achernar’s rapid rotation is typical of Be stars, but it is the only Be star for which the rotational flattening has actually been observed (Domiciano de Souza et al. 2003). Domiciano de Souza et al. (2012) revisited the star, and based on more interferometric data confirmed the initial findings of Achernar rotating at about 95% of the critical velocity. However, the determinations of the actual projected rotational speed differ quite widely: Vinicius et al. (2006) obtained $v \sin i = 223 \pm 15 \text{ km s}^{-1}$, while Domiciano de Souza et al. (2012) give $292 \pm 10 \text{ km s}^{-1}$.

Achernar is also known to be a non-radial pulsator, with a pulsation frequency of $F_1 = 0.775 \text{ c/d}$, which is both seen in spectroscopy and photometry (Rivinius et al. 2003, and references therein). A somewhat more detailed picture was obtained by Goss et al. (2011) based on satellite photometry. They found the above mentioned period to be stable in value and phase, but in amplitude being correlated with the circumstellar activity state, i.e., when circumstellar emission is present, the amplitude is high. A stronger, secondary frequency F_2 , at a value about 10% lower, was found to be present only at times of circumstellar activity, which is not atypical of Be stars (Štefl et al. 1998).

2. Observations

High-quality echelle spectra are required for the intended analysis. The data sets available for this study (see Table 1) were obtained with the instruments HEROS (Stahl et al. 1995), FEROS (Kaufer et al. 1999), UVES (Dekker et al. 2000), and HARPS (Mayor et al. 2003). Spectra taken after the year 2000 are avail-

* Based on observations collected at the European Southern Observatory at La Silla and Paranal, Chile, Prog. IDs: 62.H-0319, 64.H-0548, 072.C-0513, 073.C-0784, 074.C-0012, 073.D-0547, 076.C-0431, 077.D-0390, 077.D-0605, and the technical program IDs 60.A-9120 and 60.A-9036.

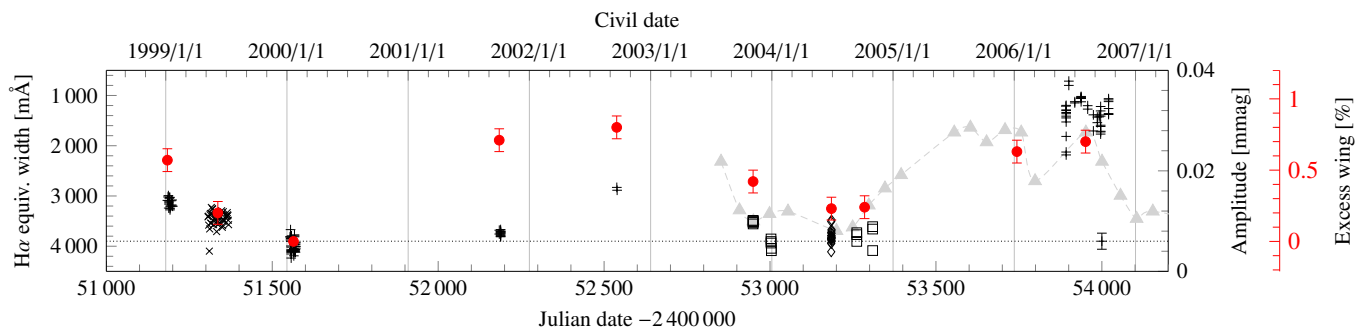


Fig. 1. Achernar $H\alpha$ equivalent width 1999 to 2007. + for FEROS, \times for HEROS, \square for HARPS, and \diamond for UVES. The mean value in diskless state, 3900 mÅ, is indicated as dotted line, the mean uncertainty of ± 160 mÅ, estimated as RMS in diskless state, is shown exemplarily in the lower right corner. Light grey triangles (\blacktriangle) are photometric amplitudes of frequency F_1 taken from Fig. 4 of Goss et al. (2011). Solid disks (\bullet) mark the depth of the excess wing signature in He I 4471 (average of red and blue side, see also Fig. 3) in the mean difference spectra.

able from the ESO Science Archive Facility. HEROS technical parameters, observing procedures, and data reduction are described by Stahl et al. (1995), UVES and FEROS data were reduced with the standard data reduction systems provided by ESO, for HARPS the reduced data were obtained from the archive. Some spectra were discarded for quality reasons or unsuitable observing modes, e.g., HARPS spectra taken with iodine cell. See Appendix A for a discussion of stability over several seasons and instruments. $H\alpha$ equivalent widths were then measured in each spectrum (Fig. 1). For the analysis of high quality differences between the seasons, the spectra in each run listed in Table 1 were averaged. **Unity was added to the difference spectra, so that the continuum has a value of one instead of zero.**

3. Variations Relative to the Diskless State

3.1. Circumstellar Contributions

Strong emission lines have never been observed in Achernar ($H\alpha$ peak height always $\lesssim 1.5 F_{\text{cont}}$, see Vinicius et al. 2006), but even these completely vanished between July and October 1999: Spectra taken with FEROS in January, 1999 and May–July, 1999 with HEROS show weak emission in $H\alpha$ only, which had fully disappeared when the star was observed in January, 2000 with FEROS again. The independent FEROS observations by Vinicius et al. (2006) were taken in October 1999 and confirm the absence of any detectable disk. Taking the spectra of Jan. 2000 as photospheric reference, one can construct the differences to test circumstellar contribution or photospheric change against

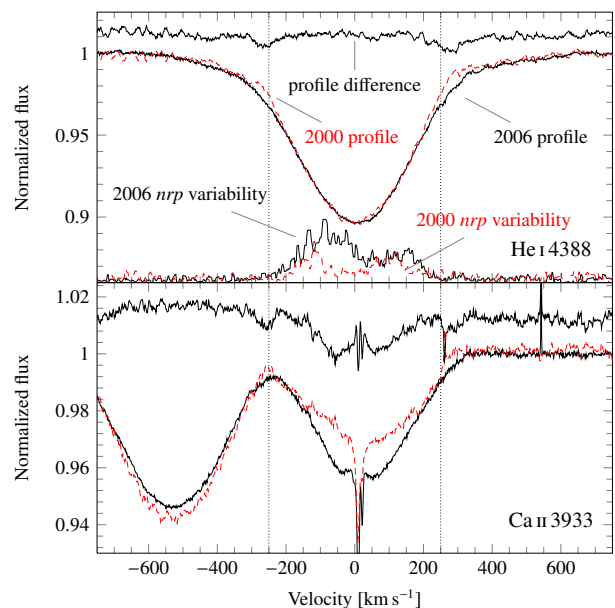


Fig. 2. FEROS 2000 (dashed, red in online version) and UVES 2006 (solid) spectra and their differences. Shown are a purely photospheric line (He I 4388) and a line with circumstellar contribution (Ca II 3933). The temporal variance spectra for the 2000 and 2006 seasons are shown for He I 4388 as well (arbitrary scaling). In neither season the pulsational power reached beyond ± 250 km s $^{-1}$ (dotted lines). The CQE in Ca II 3933 is embedded in a shell absorption (plus the interstellar line), but the additional absorption at high velocity is photospheric in both lines.

Table 1. Observations used in this work

Date range	Instrument	Coverage [nm]	Resolv. power	# of spectra
Jan. 1999	FEROS	370–890	48 000	20
Jun./Jul. 1999	HEROS	350–860	20 000	43
Jan. 2000	FEROS	370–890	48 000	44
Oct./Nov. 2001	FEROS	370–890	48 000	16
Sep. 2002	FEROS	370–890	48 000	3
Sep.–Dec. 2003	HARPS	380–690	115 000	11
Jun. 2004	UVES	320–950	60 000	17
Sep./Oct. 2004	HARPS	380–690	115 000	6
Jan. 2006	UVES	380–500	60 000	60
Jun.–Dec. 2006	FEROS	370–890	48 000	45

this reference. By the end of 2001 a weak disk had started forming (although in EW, Fig. 1, the new emission is balanced by simultaneous shell absorption, it is clearly seen in the difference spectrum, see appendix B), that peaked in 2002, was almost gone again by the end of 2003, and had completely vanished by mid 2004. Thereafter there are no spectra until 2006, by when a fully developed disk was present. It is interesting to compare this evolution to the report by Goss et al. (2011): The photometric amplitudes of the two observed frequencies follow the same pattern (see Fig. 1).

The spectra taken in 2006, towards the end of a disk formation phase, i.e., when the disk had reached maximum emission, show some properties normally only seen in shell stars. The inclination values given by modeling ($\sim 78^\circ$ by Domiciano de

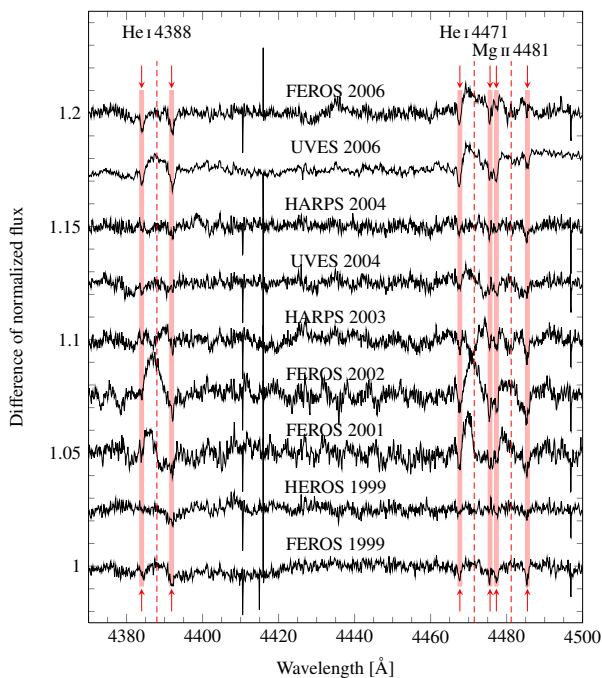


Fig. 3. Temporal evolution of the differences w.r.t. the pure photosphere state of 2000 (see as well Fig. 1). Data were averaged for each observing epoch. In seasons with only few observing epochs (FEROS 2001, 2002, and HARPS 2003) residual pulsational profile distortions are clearly seen in the line cores. Mg II 4481 shows circumstellar absorption in HARPS 2003, UVES 2006, and FEROS 2006, similar to the CQE seen in Fig. 2. Rest wavelengths of spectral lines are indicated with a dashed line, excess wing signature depression marked with arrows.

Souza et al. 2012, $\sim 65^\circ$ by Carciofi et al. 2007) are rather large, but not equatorial, suggesting that Achernar might be a transition case between clear shell and clear non-shell star. Indicators for a shell-star nature of Achernar are 1) central quasi-emission components (CQE, Rivinius et al. 1999), easily seen in Ca II 3933 (see Fig. 2) and Mg II 4481, and 2) differences from the photospheric spectrum of 1999/2000 below zero in the center of lines most easily affected by circumstellar material. The circumstellar nature of these signatures is corroborated by comparison with the modeled differences below, which, not counting the Balmer emission, do not reproduce well the core of these, and only these, lines.

3.2. Photospheric Variations

The largest circumstellar variations are present in 2006. Apart from clear double peaked emission and shell absorption contributions in the usual lines (Balmer, lowly ionized metals), however, there is a third type of difference, which is not restricted to lines typically formed in the circumstellar environment, but is seen in purely photospheric lines, too, like the He I lines in the blue part of the spectrum (see Fig. 2 for He I 4388): In the UVES 2006 data, that line shows a shallower core, but excess wings, not just deeper, but reaching out a bit farther than in 2000. In other words, the photospheric line is broader in 2006 than it is in 2000. The excess wing signature is as well seen in Ca II 3933 in Fig. 2, at higher velocity than the circumstellar shell absorption.

The pattern visible in Fig. 2 is not only seen in all He I and the Ca II lines, but also in Mg II 4481 (see Fig. 3), Si II 4128/32 doublet (see Fig. 4), and as well in C II 4267, Fe II 5169, Si II 6347/71,

or, in short, in basically all lines detected in the spectrum with a depth larger than a few percent, with the notable exception of Si III 4553. The changes of the Balmer wings seen in Fig. 4 are probably real as well; they are consistently present in all Balmer lines except H α .

This excess broadening of all photospheric lines changes on a time scale of months to years. The temporal evolution is shown in Fig. 3: In all epochs the excess outer wings (see Fig. 2) are deeper than in the diskless state observed with FEROS in 2000. The lines are narrowest when the star has no circumstellar disk. Indeed, the differences are quite small, there is almost no excess broadening in the HEROS 1999 data, and quite little in the 2004 data, all with little to no sign of a disk. The excess broadening is strongest, i.e., clearly seen deeper and wider line wings, indicated in the difference spectra by “dents” at about $v \pm 275 \text{ km s}^{-1}$ of each line, when the disk strength is increasing or steady (2001/2, 2006). When the disk strength is decreasing, the excess broadening weakens (1999 and 2003). However, as 2004 data show, the excess broadening can still be weakly present when no disk emission or shell absorption can be detected anymore.

3.3. Proof-of-Concept Modeling

Since the variation is present in almost all photospheric lines in the same manner (Si III 4553 can be explained by its polar formation locus), a change of the surface velocity field from epoch to epoch is a strong possibility. The variable pulsation amplitude, known from photometry, is one possibility. However, an inspection of the individual spectra does not support this hypothesis. The pulsational variations shown in an RMS variation analysis are well contained inside $\pm 250 \text{ km s}^{-1}$ for the 2006 season, and even within $\pm 220 \text{ km s}^{-1}$ for the 2000 season. Since that means there is no variability outside that velocity, this cannot cause excess wings observed between 250 and 300 km s^{-1} (see Fig. 2). Pairwise differences between individual high-quality spectra do as well not show any indication of the excess broadening to vary as part of the clearly seen pulsational phase differences.

This variation of the excess broadening might instead come from the photospheric rotational velocity field itself being different. As a proof of concept for this hypothesis a set of photospheric model spectra was calculated with Bruce3 (see Rivinius et al. 2013b, for a description and references). Model parameters were taken from published sources: $R_{\text{pole}} = 8 R_{\odot}$, $i = 78^\circ$, $T_{\text{eff}} = 15000 \text{ K}$ from Domiciano de Souza et al. (2012), while the mass was somewhat increased from their value of $M = 6.1 M_{\odot}$ to $M = 8.1 M_{\odot}$ to avoid the problem of interpolating equatorial local atmosphere parameters outside the grid of model spectra available for Bruce3. It should be noted that the models used are strictly models for the photospheric appearance only, so that a higher mass does not affect luminosity, etc., as it would in a model including the stellar interior. Only the local gravity, the geometric distortion, and the amount of gravity darkening are changed. Standard gravity darkening with $\beta = 0.25$ was adopted (see Appendix C for a discussion of lower β). Spectra were computed incrementing $v \sin i$ in steps of 5 km s^{-1} , from 250 to 300 km s^{-1} .

Figure 4 shows the model spectrum for $v \sin i = 250 \text{ km s}^{-1}$. At the scale of the figure, models computed with higher $v \sin i$ look virtually identical. The difference spectra, however, exhibit pronounced features, which are surprisingly close to the observed ones, given that no sort of fitting beyond selecting an appropriate $\Delta v \sin i$ was attempted. The strongest discrepancies between modeled and observed difference spectra are the above

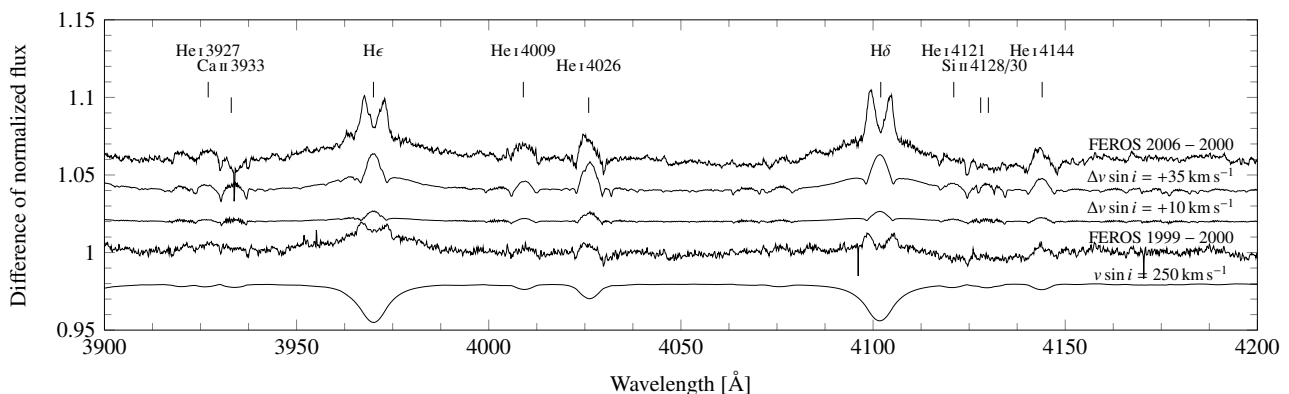


Fig. 4. As a proof of concept for a variable $v \sin i$ parameter, the differences of the FEROS 1999 and the FEROS 2006 to the FEROS 2000 spectrum are shown. Below is the modeled spectrum (scaled by a factor of 1/15), calculated with a fixed $T_{\text{eff}} = 15\,000\text{ K}$, $\beta = 0.25$, $v \sin i = 250\text{ km s}^{-1}$. The model differences of $\Delta v \sin i = +35\text{ km s}^{-1}$ and $\Delta v \sin i = +10\text{ km s}^{-1}$ are shown between the observed ones.

identified circumstellar absorption/emission effects, which are not included in the model. Equatorially formed lines, such as singly ionized metals, are affected differently than helium lines formed all over the star: In the equatorially formed lines, the excess wings are very strong, but the core remains largely unaltered, while both excess wings and line core change for He I lines. The more polar Si III 4553 line does not change at a detectable level at all. The Balmer line wings, finally, are less deep in the rapidly rotating model due to the lower equatorial gravity. All this can be understood in terms of the formation regions of the respective lines, as illustrated in Fig. 6 of Rivinius et al. (2013a): The effects of varying $v \sin i$ are the strongest at equatorial latitudes. This as well explains why, contrary to classical assumption, changes in $v \sin i$ do affect the equivalent width.

The observed time-dependent line broadening can be well explained by variations of the (equatorial) rotational velocity.

4. Discussion and Conclusions

High-quality spectroscopy of Achernar has shown a variable width of the photospheric lines. The width correlates with the disk emission. The variation can be interpreted as a change of the stellar rotation speed, and a proof-of-concept model with $\Delta v \sin i \leq 35\text{ km s}^{-1}$ matches the observations already reasonably well without parameter fitting. Such a velocity differential, on top of 95% of critical rotation, could make quite a difference for disk formation. However, the absence of a detectable spin-up *before* the onset of disk formation, marked by photometric amplitude increase in Fig. 1, puts constraints on models that first transport angular momentum upwards into the outer photosphere, and then “offload” this angular momentum excess into a circumstellar disk. Instead, the excess width correlates with the *presence and decay* of the disk.

In a viscous disk scenario, “decay of the disk” actually means that disk material is being reaccreted onto the central star. Even in build-up and steady-state feeding phases, the very nature of viscous angular momentum transport requires that some fraction of the material in the inner disk is reaccreted. A temporary accretional spin-up of the equatorial surface region only is a possible hypothesis: The enhanced velocity is dissipated back into deeper stellar regions after the reaccretion ceases, and the angular momentum required for disk formation may be taken from such deeper seated regions instead of the photospheric surface.

In any case, current models for stellar photospheres do not handle such a situation well. For instance, instead of keeping T_{eff} constant with the spin-up, one could as well keep either the polar temperature or the luminosity constant; or implement an equatorially enhanced differential rotation and correspondingly modified local gravity/temperature values instead of a solid body spin-up; or change the values of gravity darkening and/or equatorial temperature. However, to explore and lift these possible degeneracies is well beyond the scope of this discovery report.

Since about January 2013 Achernar has been building up a new disk from almost zero emission (T. Napoleão & R. Marcon, priv. comm., 2013). With Achernar being the closest and apparently brightest Be star, this offers a timely opportunity to obtain dedicated observations, and to scrutinize whether the spin-up is cause or consequence of disk formation. Similar findings for other Be stars might be waiting for discovery in archival data.

Acknowledgements. RHDT acknowledges support from NASA award NNX12AC72G. ACC acknowledges support from CNPq (307076/2012-1) and Fapesp (2010/19029-0). The referee has greatly helped to improve the robustness against potential objections.

References

- Ando, H. 1986, *A&A*, 163, 97
 Carciofi, A. C., Magalhães, A. M., Leister, N. V., Bjorkman, J. E., & Levenhagen, R. S. 2007, *ApJ*, 671, L49
 Dekker, H., D’Odorico, S., Kaufer, A., Delabre, B., & Kotzlowski, H. 2000, in *SPIE Conf. Ser.*, ed. M. Iye & A. F. Moorwood, Vol. 4008, 534
 Domiciano de Souza, A., Hadjara, M., Vakili, F., et al. 2012, *A&A*, 545, A130
 Domiciano de Souza, A., Kervella, P., Jankov, S., et al. 2003, *A&A*, 407, L47
 Goss, K. J. F., Karoff, C., Chaplin, W. J., Elsworth, Y., & Stevens, I. R. 2011, *MNRAS*, 411, 162
 Haubois, X., Carciofi, A. C., Rivinius, T., Okazaki, A. T., & Bjorkman, J. E. 2012, *ApJ*, 756, 156
 Kaufer, A., Stahl, O., Tubbesing, S., et al. 1999, *The Messenger*, 95, 8
 Mayor, M., Pepe, F., Queloz, D., et al. 2003, *The Messenger*, 114, 20
 Neiner, C., Mathis, S., Saio, H., & Lee, U. 2013, in *Progress in Physics of the Sun and Stars: A New Era in Helio- and Asteroseismology*, ed. H. Shibahashi & A. E. Lynas-Gray, ASPC, in press
 Rivinius, T., Baade, D., & Štefl, S. 2003, *A&A*, 411, 229
 Rivinius, T., Carciofi, A. C., & Martayan, C. 2013a, *A&A Rev.*, submitted
 Rivinius, T., Townsend, R. H. D., Kochukhov, O., et al. 2013b, *MNRAS*, 429, 177
 Rivinius, T., Štefl, S., & Baade, D. 1999, *A&A*, 348, 831
 Rogers, T. M., Lin, D. N. C., McElwaine, J. N., & Lau, H. H. B. 2013, *ApJ*, 772, 21
 Stahl, O., Kaufer, A., Wolf, B., et al. 1995, *Journal of Astronomical Data*, 1, 3
 Štefl, S., Baade, D., Rivinius, T., et al. 1998, in *ASPC, Vol. 135, A Half Century of Stellar Pulsation Interpretation*, ed. P. A. Bradley & J. A. Guzik, 348
 Vinicius, M. M. F., Zorec, J., Leister, N. V., & Levenhagen, R. S. 2006, *A&A*, 446, 643

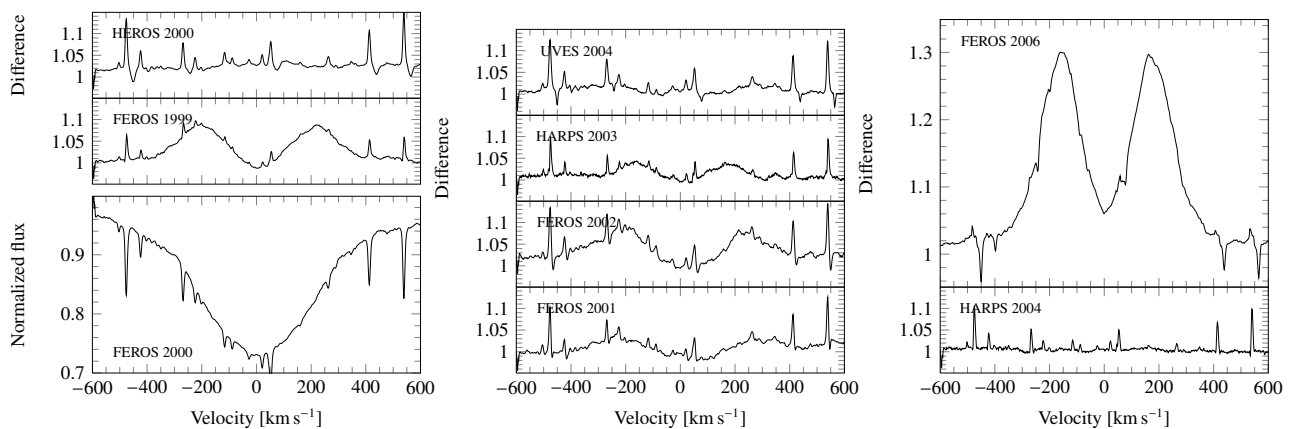


Fig. B.1. $H\alpha$ difference profiles w.r.t. FEROS 2000 for all observing seasons. Telluric lines were not corrected for.

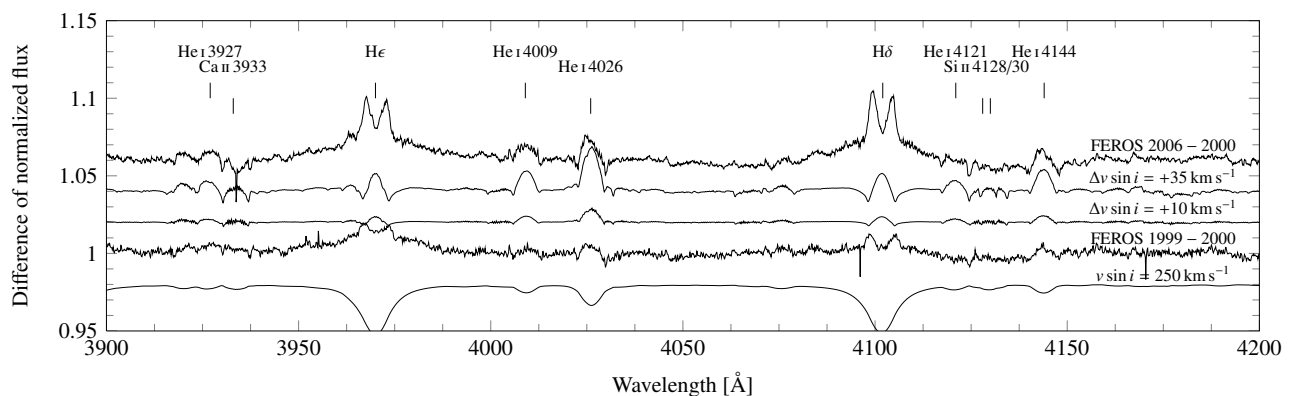


Fig. C.1. Same as Fig. 4, with models computed for a fixed $T_{\text{pole}} = 16900$ K and $\beta = 0.20$.

Appendix A: Cross-Season and -Instrument Data

Using data from four different instruments, over about a decade, in order to detect subtle effects might be problematic in terms of stability and cross-instrumental effects. All are echelle spectrographs; HARPS, FEROS and HEROS are attached by fiber-link, UVES is mounted on a gravity invariant Nasmyth platform. The three ESO instruments are monitored, and partly thermally controlled, for stability. All spectra were used in the heliocentric reference frame. The pixel sampling of the spectra is from 0.1 \AA (HEROS) over 0.03 \AA (FEROS) down to about 0.01 \AA (UVES and HARPS). This is much smaller than the width of the observed variations, which are several tens of km s^{-1} even for the most narrow ones, the high velocity “dents”. The observed line depths differ by almost 2% of the continuum, at a typical S/N of the average spectra of about 1000. The observed effect is not systematically different between FEROS–FEROS and OTHER–FEROS comparisons.

As the variations are well oversampled and have a consistent appearance and evolution through all data sets, regardless of instrument, a cross-instrumental/stability effect can be excluded.

Appendix B: The $H\alpha$ Difference Spectra

To allow an assessment of the circumstellar disk strength independent of the $H\alpha$ equivalent width, the seasonal $H\alpha$ profiles are shown in Fig. B.1 in a similar format as given by Vinicius et al. (2006) in their Fig. 12. In a shell star, the net effect of a weakly

developed disk on the overall $H\alpha$ equivalent width can vanish if, as happened in Achernar in 2001, the contributions from line emission and shell absorption just cancel one another. Note as well the unusual Balmer-line CQE seen in the FEROS 2001 and somewhat more strongly in UVES 2004 data.

Appendix C: The Gravity Darkening Parameter

In the proof-of-concept model a gravity darkening value of $\beta = 0.25$ was used, even though lower values of β are typically derived observationally. We note that $\beta = 0.2$ was adopted by Domiciano de Souza et al. (2012), though not derived. The model we use can compute spectra for different values of β , but the current formalism to compute the corresponding stellar parameters, in particular T_{eff} and L , has been derived with a fixed $\beta = 0.25$. For this reason, modeling with a fixed T_{eff} is only possible with $\beta = 0.25$, a shortcoming that will be overcome in a more detailed dedicated work. To demonstrate that the effect does not vanish for a different β , we show models computed with constant T_{pole} instead, for $\beta = 0.20$ (Fig. C.1). Compared to the models shown in Fig. 4, the “dents” are unaltered in Ca II 3933 and the Si II lines, and slightly less pronounced in He I lines, but still clearly present in He I 3927, 4009, 4121, 4144. The most significant difference is that the Balmer line wings are not reproduced any more (and Balmer lines are generally stronger), which, however, is an effect dominated by keeping T_{pole} fixed rather than T_{eff} , and unrelated to the value of β .